

## Extrinsic photoconductivity in poly(3-dodecylthiophene) sandwich cells

S. B. Lee\* and K. Yoshino

*Department of Electronic Engineering, Faculty of Engineering, Osaka University, 2-1 Yamada-Oka, Suita, Osaka 565-0871, Japan*

J. Y. Park and Y. W. Park

*Department of Physics and Condensed Matter Research Institute, Seoul National University, Seoul 151-742, Korea*

(Received 19 March 1999; revised manuscript received 30 July 1999)

We have measured the photocurrent action spectra of the Al/poly(3-dodecylthiophene)(P3DDT)/ITO and Au/P3DDT/ITO sandwich cells. The photoinjection from both ITO and Au electrodes was observed at room temperature. No polarity effect was found in the ITO/P3DDT/Au device at low temperatures. The photoinjection from ITO electrode is found not effective at low temperatures. The photocurrent at low temperatures was attributed to photoinjection from Au electrode at both polarity of bias voltage. A phenomenological model of photoconductivity in poly(3-dodecylthiophene) sandwich cells at low-electric fields and low temperatures is proposed. An approach for photoconductivity enhancement in conducting polymers is discussed.

### I. INTRODUCTION

There is a great deal of interest to the mechanism of charge photogeneration, separation, and transport in  $\pi$ -conjugated polymers.<sup>1-8</sup> Junction devices utilizing semi-conducting polymers as active material have been considered to be a candidate for highly efficient low cost solar cell. The discovery of electroluminescence in poly(p-phenylenevinylene) has excited the new surge of interest to the  $\pi$ -conjugated polymer materials and raised the problems that have not been resolved earlier. Among them the studies of the electrode/polymer interface are of great importance for understanding the fundamental processes in these materials and developing polymer devices with improved performance.<sup>9</sup> The importance of extrinsic effects and interchain coupling for charge-carrier photogeneration has been understood due to the intensive studies during the last years.<sup>3-6,10</sup> However, the picture is rather complex because of a complicated structure of every individual polymer material, an inevitable various defects and unintentionally introduced impurities, the effect of photoinjection from electrodes, and the large difference of hole and electron mobilities.

The general scheme of the charge-carrier generation processes in nondegenerated conjugated polymers was discussed in detail recently.<sup>6</sup> Positive mobile charge carriers responsible for the photocurrent are produced by the dissociation of primarily singlet-excited species by oxygen,<sup>4,6,10</sup>  $C_{60}$  (Ref. 11) or other acceptor-type products.<sup>10</sup> Another channel of charge-carrier photogeneration is the dissociation of interchain polaron pairs (singlet as well as triplet) formed by interchain charge transfer from singlet excitons.<sup>3,12</sup> Under the terms "intrachain" and "interchain" we mean "within the same conjugation length" and "between different conjugation length on the same chain as well as on different chains," correspondingly, as one was formulated in Ref. 12. Polaron pairs can be photoexcited either on one chain by photons with energy much higher than the absorption edge<sup>7</sup> or on adjacent chains with the formation of interchain excitons. These polaron ( $P^\pm$ ) pairs can also evolve to bipolarons

( $BP^{2\pm}$ ). Direct reaction  $P^\pm + P^\pm = BP^{2\pm}$  is hindered by strong Coulomb repulsion, but the residual impurities and dopants can facilitate this process.<sup>13</sup>

Interchain interactions determine many photoelectronic processes in conjugated polymers: the photogeneration and separation of interchain polaron pairs, the stability of photoexcited excitonic states and the dissociation of intrachain/interchain excitons.<sup>14-16</sup> This is the reason why polythiophene derivatives with variable length of side chains are one of the most attractive conjugated polymers.<sup>16-19</sup>

The effect of alkyl side groups on the photoluminescent and electroluminescent properties of poly(3-alkylthiophene) (P3AT) has been investigated earlier.<sup>17</sup> The nature of photoluminescence in P3AT is primarily due to intrachain exciton decay with a natural lifetime of about 1 ns. It has been shown that the higher photoluminescent and electroluminescent intensities are obtained by increasing the alkyl side chain length.<sup>17</sup> This is explained by the confinement of carriers on a main chain of P3AT due to the longer interchain distance for longer alkyl side chains.

In this paper, we present the results of the study on the photocurrent action spectra of the Al/P3DDT/ITO and Au/P3DDT/ITO sandwich cells. The temperature-dependent photoinjection from the ITO and Au electrodes in this device is discussed and the phenomenological model of photoconductivity in poly(3-dodecylthiophene) sandwich cell at low-electric field, low temperatures, and low-light intensities is proposed.

### II. EXPERIMENT

Poly(3-dodecylthiophene) was prepared by the method already reported.<sup>20</sup>

We have studied the sandwich structure. The P3DDT layer was fabricated by spin coating a chloroform solution of P3DDT on patterned ITO-coated glass substrate. Then the aluminum or gold semitransparent electrode was evaporated through a shadow mask with an active area of 1 mm<sup>2</sup>. The thickness of P3DDT was measured by Alpha-step profilometer.

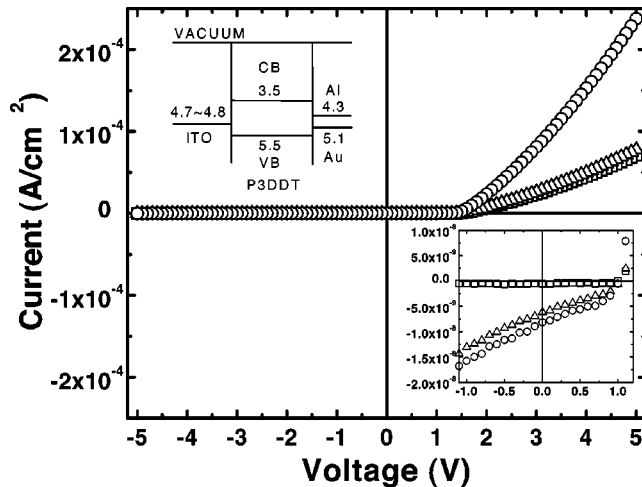


FIG. 1. Current-voltage characteristics of an Al/P3DDT/ITO structure in the dark (open square) and under illumination by light with energy of 2.1 eV (open circle) and 2.6 eV (open triangle) through Al electrode. The right insert shows enlarged J-V curves in the range  $\pm 1.0$  V. The thickness of P3DDT film is 0.2  $\mu\text{m}$ . The electronic energy level scheme is shown on the left insert.

Current-voltage characteristics were measured by a Keithley 487 picoammeter with a built-in voltage source. We shall use the expression “positive/negative bias” through the text, which means a positively/negatively biased ITO electrode. As an excitation source we used a calibrated Xenon lamp. The spectral dependence of photocurrent was measured by a standard phase sensitive lock-in detection method using a EG&G 5208 two-phase lock-in analyzer at a low-mechanical chopper frequency of 17 Hz and a Keithley 228A voltage/current source. The dual-phase lock-in analyzer has enabled us to measure both the magnitude of the signal as well as the phase. In independent experiments, we have also controlled the in-phase signal. Photoelectrical measurements were carried out in a vacuum temperature-controlled optical cryostat in vacuum  $< 10^{-3}$  mbar. The absorption spectra were measured using a Beckman DU-70 spectrophotometer. Experimental details about device structure and measurement are discussed below along with the results.

### III. RESULTS

#### A. Al/P3DDT/ITO

The current-voltage (J-V) characteristics of the Al/P3DDT(0.2  $\mu\text{m}$ )/ITO structure in the dark (open squares) and under light illumination through semitransparent Al-electrode at photoexcitation energy of 2.6 eV (open triangles) are plotted in Fig. 1. This Schottky type rectifying J-V characteristic can also be found in many early papers on polymeric photodiodes.<sup>21</sup> Upon illumination of strongly absorbed light many authors have observed the enhancement of the photocurrent at negative bias and only small (negligible) enhancement at positive bias.<sup>22</sup> But in many cases, the enhancement of photocurrent at positive bias has been emphasized.<sup>5,23,24</sup> This differentiates the organic photodiodes from conventional inorganic semiconductor photodiodes.<sup>25</sup>

Figure 1 shows such anomalous type of the J-V characteristic for the same Al/P3DDT/ITO structure upon illumina-

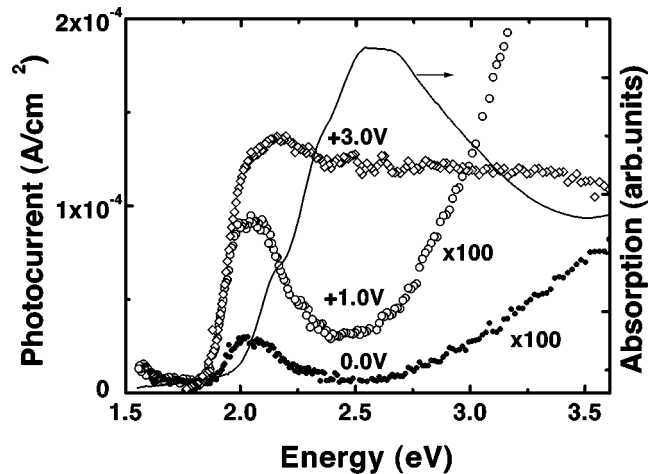


FIG. 2. Spectral characteristics of photocurrent of Al/P3DDT/ITO structure at different positive biases (0.0 V; +1.0 V and +3.0 V).

tion through the semitransparent Al-electrode with weakly absorbed light with photon energy of 2.1 eV (open circles). The photocurrent for both photoexcitation energies (2.1 and 2.6 eV) was normalized to the same intensity of incident light. The most remarkable feature in Fig. 1 is the significant growth of photocurrent with increase of positive voltage at photoexcitation energy of 2.1 eV. It is clearly seen that both curves are very close to each other at negative bias but begin to diverge at positive bias, when the applied voltage exceeds the built-in potential value (the open circuit voltage  $U_{oc} \approx 1.0$  V). This voltage corresponds to the vanishing of a barrier and the beginning of charge carrier injection from electrodes. On the right insert of Fig. 1 the enlarged J-V characteristics are shown in the voltage range of  $\pm 1.0$  V. The electronic energy level scheme of Al(Au)/P3DDT/ITO heterostructure is shown on the left insert. The ionization potential of P3DDT was determined by cyclic voltammetry.<sup>26</sup> The work function of ITO was taken from Ref. 9 and the metal work functions from Ref. 27.

Figure 2 shows the spectral characteristics of the photocurrent of Al/P3DDT/ITO structure under illumination through ITO-electrode at different voltages. We should remind here that we plotted the magnitude of photocurrent on spectral characteristics, i.e., the absolute value, and illumination in this case was through ITO electrode. The broad spectral photoresponse was observed at positively biased ITO-electrode (+3.0 V). But at low-positive voltages below +1.0 V the photoresponse at the photon energy around absorption peak was much suppressed and two side bands of opposite phase appeared. The absorption spectrum of the thin film of P3DDT is shown for comparison.

Taking into consideration that the major charge carriers in P3DDT are holes as well as in most other semiconducting polymers and to simplify the problem by excluding the effect of electron injection and the influence of chemically modified intermediate layer between Al electrode and polymer<sup>9,28</sup> we have further studied the “hole-only” Au/P3DDT/ITO device. The replacement of the low work-function Al electrode (4.3 eV) with higher work-function Au electrode (5.1 eV) significantly reduces the number of injected electrons. The thickness of P3DDT film in this case was about 2  $\mu\text{m}$ .

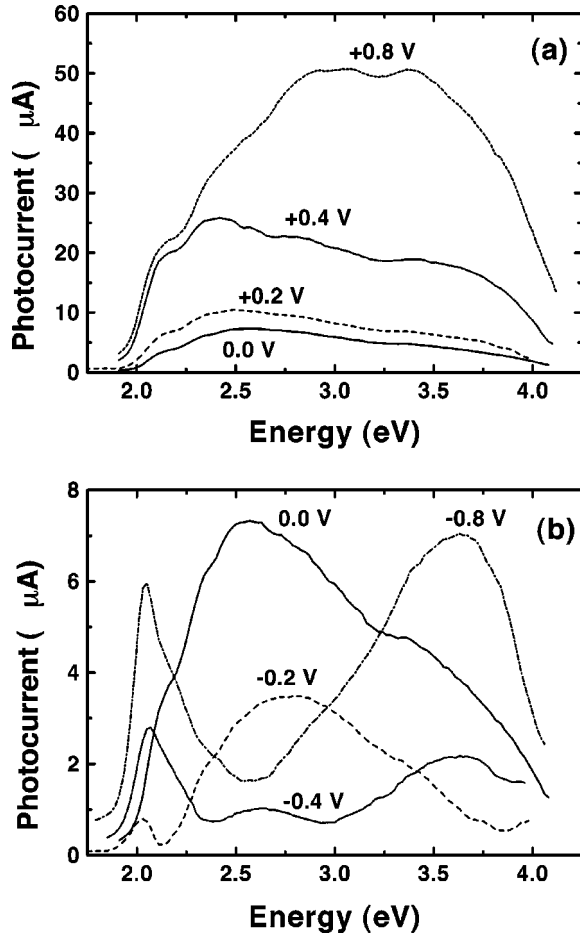


FIG. 3. Dynamics of spectral changes of photocurrent in the Au/P3DDT/ITO heterostructure at low voltages at room temperature: (a) positive bias; (b) negative bias. The thickness of P3DDT film is about  $2 \mu\text{m}$ .

### B. Au/P3DDT/ITO

We have measured the spectral characteristics of photocurrent in the Au/P3DDT/ITO heterostructure [Figs. 3(a) and 3(b)] at low voltages at room temperature. The magnitude of photocurrent signal is plotted for convenience of comparison. A broadband spectral photoresponse was observed at positive polarity of voltage applied to the ITO electrode. The photoresponse was increased with the increase of positive voltage [Fig. 3(a)]. On the other hand, at negative voltage the wide central band was suppressed but then two new side bands appear [Fig. 3(b)]. That is, the wide central band completely disappears and only two new strong side bands remain at voltage of about  $-0.5 \text{ V}$ , which still grow with increasing negative voltage. This voltage is close to the difference in the work functions of Au ( $5.1 \text{ eV}$ ) and ITO ( $4.7 \text{ eV}$ ).

The most interesting results were obtained during the study of the temperature dependence of the photocurrent spectra in  $100\sim 300 \text{ K}$  range. Figures 4(a) and 4(b) show the spectral dependence of photocurrent in Au/P3DDT/ITO structure upon illumination through the ITO electrode at  $+10 \text{ V}$  (a) and  $-10 \text{ V}$  (b) at various temperatures ( $\pm 10 \text{ V}$  corresponds to electric field of  $\pm 5 \times 10^4 \text{ V/cm}$ ). All spectra were normalized to the same light intensity.

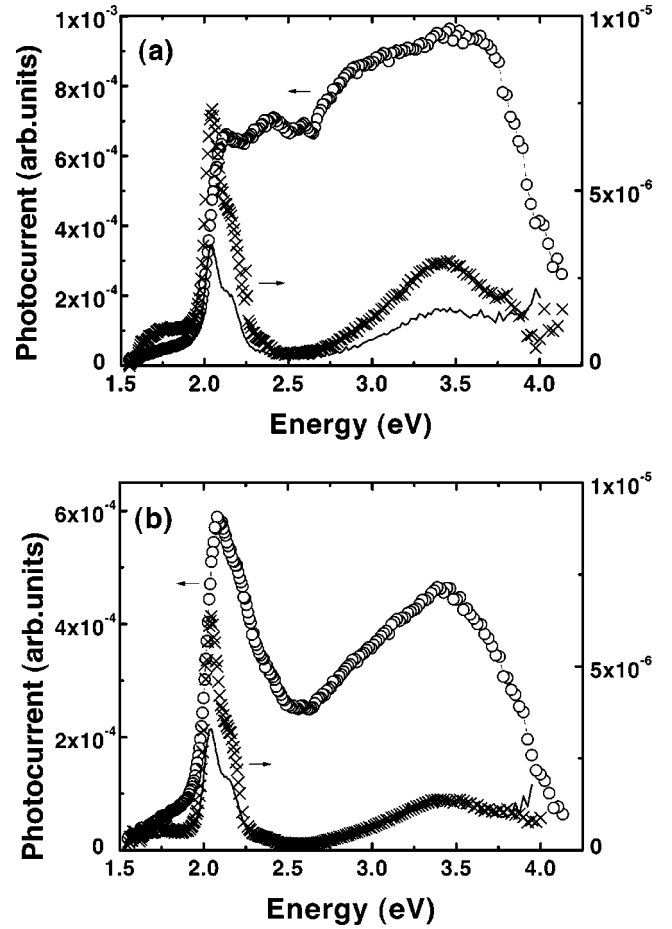


FIG. 4. Spectral dependence of photocurrent in Au/P3DDT/ITO structure upon illumination through the ITO-electrode at  $+10 \text{ V}$  (a) and  $-10 \text{ V}$  (b) at different temperatures (open circle -  $290 \text{ K}$ , cross -  $130 \text{ K}$ , solid line -  $107 \text{ K}$ ).  $\pm 10 \text{ V}$  corresponds to electric field of  $\pm 5 \times 10^4 \text{ V/cm}$ .

No polarity effect has been found at low temperatures contrary to the results at room temperatures. By comparing Figs. 4(a) and 4(b) it is clearly seen that in the case of negative bias the shape of photocurrent spectrum does not change with decrease of temperature, but the total decrease of photocurrent was only observed. On the other hand, in the case of the positive bias the spectral shape changes very much with temperature. The strong photoresponse in the broad spectral range was observed at room temperature but not at low temperature. The temperature dependence of the photocurrent of Au/P3DDT/ITO structure excited with light of  $\lambda_1 = 476 \text{ nm}$  ( $2.1 \text{ eV}$ ) and  $\lambda_2 = 592 \text{ nm}$  ( $2.6 \text{ eV}$ ) is shown in Fig. 5. The temperature dependence of both components of photocurrent is non-Arrhenius like.<sup>5</sup> The photoconductivity increases with the temperature, showing an activation-type behavior above about  $200 \text{ K}$ . We can see in the plot, that the photocurrent generated by low-energy photon is less temperature dependent and decreases more slowly with decreasing of temperature than that by the higher photon energy. We have estimated the activation energy in high-temperature range where the space charge effects is small, to be  $E_1 = 0.17 \text{ eV}$  for the former and  $E_2 = 0.25 \text{ eV}$  for the latter.

We have measured the temperature dependence of dark J-V characteristics of Au/P3DDT/ITO device (Fig. 6). At room temperature the dark J-V characteristic is almost

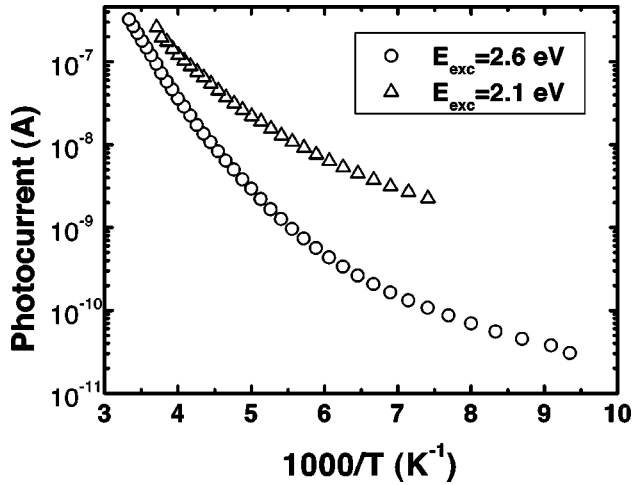


FIG. 5. Temperature dependence of the photocurrent of Au/P3DDT/ITO structure under illumination with light of  $\lambda = 476$  nm (2.1 eV) and 592 nm (2.6 eV).

linear at low-electric field. At low temperatures we have observed the superlinear J-V characteristics at a field  $\geq 5 \times 10^4$  V/cm and the J-V characteristic could be approximated by power law  $J \propto V^n$  with  $n \approx 3$ , which is a similar characteristic with those of space charge limited current (SCLC) with the traps in energy gap.<sup>29</sup>

#### IV. DISCUSSION

##### A. Al/P3DDT/ITO

A simple spectral analysis of the first derivative of the first absorption band of P3DDT film reveals the  $S_0 \rightarrow S_1/0 \rightarrow 0$  broadened transition at about 2.1 eV and its phonon-side bands separated by 0.16 eV. The photoluminescence spectrum shows the similar vibronic structure. The more careful study by the electroabsorption spectroscopy<sup>30</sup> has shown the sharp derivative-like feature of  $1B_u$  exciton at low energy, followed by a series of phonon sidebands. Therefore, the dominant photoexcitation in P3DDT is exciton.

The enhancement of photocurrent with increasing negative voltage (shown on the right insert of Fig. 1) in polymeric

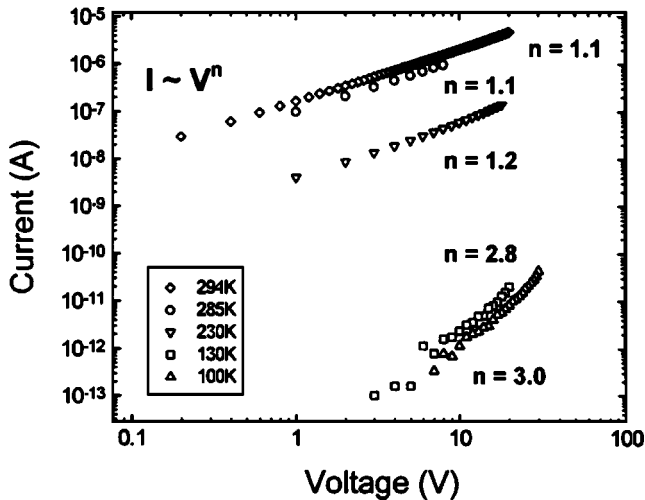


FIG. 6. Temperature dependence of dark J-V characteristics of Au/P3DDT/ITO device.

photodiode could be explained by the electric field-assisted exciton dissociation as one has been observed in experiments on electric field-induced luminescence quenching in light-emitting diodes based on poly(phenylphenylvinylene)<sup>31</sup> and ladder-type poly(p-phenylene)<sup>32</sup> and by field-dependent mobility at high-electric field.<sup>33</sup>

However, the much bigger enhancement of the photocurrent was observed at relatively low positive voltages under photoexcitation with energy of 2.1 eV through semitransparent Al electrode. This energy is slightly higher than the absorption edge of P3DDT. Therefore, there are two possible channels for the observed strong enhancement of the photocurrent at positive voltage: the bulk photoelectronic processes and the photoinjection of holes from the opposite ITO electrode into P3DDT. The experimental support for the dominant role of the photoinjection of holes from an ITO electrode into conjugated polymer have been presented by S. Barth *et al.*<sup>5</sup> The light-induced luminescence quenching by photoexcited charged polaronic states<sup>34</sup> could not explain why the photocurrent sufficiently exceeds the dark forward current. The photocurrent multiplication process proposed recently by T. K. Däubler *et al.*<sup>8</sup> cannot play any role in such low fields. The low photocurrent at positive voltage for photoexcitation with strongly absorbed light could be explained by the low dissociation rate of excitons at Al/polymer interface and the poor electron transport in P3DDT because the electron transport in conjugated polymers is strongly trap limited and the higher recombination rate at electrode/polymer interface.<sup>35</sup>

The photoelectronic processes in polymer device with asymmetric electrodes are very complicated since the photocurrent is proportional to  $n \times \mu$  product and both the carrier density  $n$  and the carrier mobility  $\mu$  depend on electric field, temperature, intensity and wavelength of light. Further elaborate studies are needed to clarify the mechanism of photogeneration and transport of charge carriers in polymeric photodiodes, especially at high-electric field.

##### B. Au/P3DDT/ITO

The experimental results for hole-only Au/P3DDT/ITO device have clearly shown the following facts: (1) the strong polarity effect at room temperature and absence of that at low temperature; (2) the strong filter effect at both polarities of applied voltage at low temperatures; (3) the activation energy of photocurrent excited by weakly absorbed light with lower energy near absorption threshold is lower than that for higher photon energy.

At room temperature the polarity effect can be explained by both the photoinjection from electrode and the large difference between the hole and electron mobilities. We should note here that the photoinjection from electrodes does not mean the injection of charge carriers by the optically excited electrode. The excitons in polymer dissociate at ITO/polymer interface by electron transfer to positive ITO electrode. The holes (positive polarons) are collected by the negative opposite electrode. In the case of negative ITO electrode the excitons dissociate by hole transfer to negative ITO electrode. The electrons have to pass through the polymer film. It is well known that electron transport in conjugated polymer is trap limited. This leads to strong polarity (filter) effect. Only the holes generated by exciton dissociation at

back Au electrode can be efficiently collected by front negative ITO electrode and contribute to photocurrent.

The absence of polarity effect and coincidence of photocurrent spectra for both polarity at low temperature means that the photoinjection from the ITO electrode does not have large effect at low temperatures. The low temperature photocurrent may characterize the bulk photoconductivity of the polymer. However, at low temperatures and low-electric field the exciton dissociation yield in the bulk is negligibly small and temperature independent.<sup>5,36</sup>

At lower temperatures the photocurrent was much suppressed because the charge carriers are trapped due to disorder effects. That is, even hole transport should be much suppressed at low temperatures. At low temperatures the charge carrier transport should be changed from the phonon-assisted polaron hopping to disorder trapping because polarons are most likely to be trapped due to disorder effects. To our knowledge, the experimental data on polaron mobility at low temperatures below 200 K are not available yet. The measurement of the temperature dependence of hole mobility in PPV derivatives was limited in a temperature range of 200–300 K where usually a thermally activated behavior is observed. Barth *et al.*<sup>5</sup> have found the non-Arrhenius-like temperature dependence of the intrinsic photocurrent in a PPV ether. Based on our experimental data on the strong filter effect and absence of polarity effect we can speculate that at low temperatures the large difference between hole and electron mobilities may disappear and could not be a reason for polarity-dependent photocurrent spectra.

The photoinjection from the electrode is determined by the diffusion length of excitons. The rate constant for exciton dissociation decreases exponentially with the distance from electrode.<sup>37</sup> At room temperature the exciton diffusion range of about 50 monomer units (20 nm) was estimated from the data on concentration dependence of photoluminescence quenching in C<sub>60</sub>-doped polymer.<sup>38</sup> The similar estimate of 20 nm was obtained for phenylene vinylene oligomer by considering the diffusion controlled photoluminescence quenching near Ca electrode.<sup>39</sup> However, the nonradiative energy transfer can occur even if the polymer is separated from metal by a transparent layer at distance as long as 60 nm from metal surface.<sup>40</sup> The exciton diffusion length obtained from experimental data on photoluminescence quenching can not be applied to the interface. For photoinjection from electrode the charge transfer is needed, and, hence, the direct contact between polymer and metal.<sup>5</sup> At low temperatures the diffusion of excitons to surface is slow. There is an increasing probability of reaction with interfacial surface states. Therefore, we assume more realistic values of 5–10 nm for exciton diffusion length.<sup>5</sup>

When diffusing exciton approaches to electrode, it dissociates at polymer/electrode interface by charge transfer to electrode resulting in a pair of charges, which consists of a hole or electron in polymer and its image charge in the electrode separated by a distance  $2r_o$ . Only the charge carriers having sufficient energy to escape recombination with the electrode could contribute to photocurrent. The fraction of these charge carriers is determined by<sup>37</sup>

$$\phi = \exp\left(-\frac{E_{coul}}{kT}\right), \quad (1)$$

where the Coulombic energy of attraction  $E_{coul}$  between the charge and its image is

$$E_{coul} = -\frac{e^2}{4\pi\epsilon\epsilon_0 r_o}. \quad (2)$$

$E_{coul}$  depends on the electric field, but in low field ( $\leq 5 \times 10^4$  V/cm) this influence is small. The measurement of temperature dependence of photocurrent has given the activation energy  $E_1 = 0.17$  and  $E_2 = 0.25$  eV at excitation energies of 2.1 and 2.6, correspondingly. The transport of charge carriers in both cases occurs in the same conditions. If the energy of exciting light would be taken into account this difference in activation energy should be of opposite sign. Higher exciting states is more likely to dissociate and contribute to photocurrent.

Therefore, this difference should reflect the difference in photoinjection properties of ITO and Au electrodes. Hence, we can make the conclusion that the photoinjection from Au electrode is more effective and the photoinjection of holes from ITO electrode is not effective at low temperatures.

Let us consider the possible reasons for difference in photoinjection properties between ITO and gold. There are several possible reasons. (1) The difference in work functions of ITO and Au is, of course, the primary reason. (2) The ITO electrode was identified as a source of oxygen<sup>41</sup> leading to a formation of carbonyl, a concomitant polymer chain scission and a loss of conjugation near interface. Therefore, a thin higher impedance intermediate oxidized layer exists at ITO/polymer interface, which could partially hinder the photoinjection from ITO electrode. Another possible reason is the indium contamination from ITO electrode.<sup>42</sup> We should also mention here that the electron injection from ITO to polymer is not efficient.<sup>5</sup>

On the basis of presented experimental results, we can propose the phenomenological model for photoconductivity in ITO/P3DDT/Au sandwich configuration at a low temperatures, a low-electric field and a low intensity of incident light. The intensity of incident light was no more than  $10^{14}$  ph/cm<sup>2</sup> in maximum of spectrum. In this model, we propose that photoconductivity in ITO/P3DDT/Au sandwich cell is an extrinsic process. It is determined by photoinjection of holes from backside Au electrode at positive bias and photoinjection of electrons from the same Au electrode at negative bias. The excitons in the bulk and near ITO electrode are mainly recombine radiatively or nonradiatively. The model is the modification of the Ghosh and Feng model.<sup>43</sup> In their model, Ghosh and Feng have used the boundary conditions  $n = 0$  at  $x = 0$  and  $x = d$ , where  $n$  is the number of excitons,  $d$  is the polymer film thickness. The number of excitons photogenerated in the region  $dx$  inside the bulk of the polymer film is

$$\phi(\alpha)N\alpha \exp(-\alpha x)dx, \quad (3)$$

where  $\phi$  is the quantum efficiency,  $N$  is the number of incident photons per square centimeter per second,  $\alpha$  is the absorption coefficient.

Harrison, Grüner and Spencer<sup>1</sup> have undertaken a quantitative examination of several different theoretical models and obtained poor fits of their experimental data by all models because all these models assume a constant spectrally-

independent photogeneration quantum efficiency. However, Binh, Gailberger, and Bässler<sup>44</sup> have noted that the excitation energy of photon is important. The linear dependence of quantum efficiency as a function of absorption coefficient was deduced from their experimental data on dc photoconductivity of P3DDT.<sup>44</sup> In  $\pi$ -conjugated polymers the excitation forms a loosely bounded  $e$ - $h$  pair ready for thermal dissociation by hopping of one of constituent charge to a neighboring site of lower ionization potential or higher electron affinity. The probability of this event is proportional to absorption coefficient in the sense that the absorption band is interpreted as an inhomogeneously broadened exciton transition and the expense of Coulombic binding energy is compensated by a gain in site energy.

The probability to have more favorable neighbors on the same chain or in adjacent chains is proportional to absorption coefficient at the absorption tail and become constant at higher photon energy.<sup>5</sup> The excess of photon energy could be transferred to hole or electron inside polymer. Hence, hole/electron could have higher probability to escape recombination with its image charge because of larger thermalization distance.<sup>5</sup> Experimental support for this also comes from the energy-dependent photoluminescence decay time.<sup>45</sup>

We should also notice here that the photoconductivity spectrum of P3DDT follows the absorption spectrum reflecting even the vibronic features. So, we assume in our simplified model of photoconductivity at low temperature, low-electric field, and low-light intensity that the quantum efficiency is proportional to absorption coefficient  $\phi \propto \alpha$  at absorption tail up to the maximum absorption energy and constant at high energy.

A space-charge limiting regime starts at  $\geq 5 \times 10^4$  V/cm in dark (see Fig. 6) and transition voltage to SCLC regime increases with increasing carrier concentration by photoabsorption. Under the assumption that at low electric field ( $\leq 5 \times 10^4$  V/cm) we are in ohmic region, for the light incident through the transparent ohmic electrode we can write:<sup>43</sup>

$$n = \int_0^d \phi(\alpha) N \alpha \exp(-\alpha x) \exp\left(-\frac{d-x}{l}\right) dx$$

$$= \phi(\alpha) N \frac{\alpha}{\alpha - \beta} [\exp(-\beta d) - \exp(-\alpha d)], \quad (4)$$

where  $l$  is the diffusion length of exciton and  $\beta = 1/l$ .

Mobility ( $\mu$ ) is constant at low-electric field and unaffected by light excitation, Therefore, a simple expression for the photocurrent for both polarity can be valid

$$j_{ph}^{\pm} = qn\mu_o U/d, \quad (5)$$

where  $\mu_o$  is the low field mobility,  $U$  is the applied voltage.

In Fig. 7(a) the photocurrent action spectrum of Au/P3DDT(2  $\mu$ m)/ITO heterostructure (cross) under illumination through ITO-electrode at  $\pm 10$  V ( $\pm 2.5 \times 10^4$  V/cm) at 130 K is shown with theoretical simulation for different exciton diffusion lengths (5 nm - solid line, 100 nm - dotted line, 200 nm - dashed line). Figure 7(b) shows the theoretical simulation of photocurrent spectrum for exciton diffusion length of 5 nm and different film thicknesses (1.6  $\mu$ m - solid line, 1.0  $\mu$ m - dotted line, 0.5  $\mu$ m - dashed line, and 0.1  $\mu$ m - dash-dotted line). The curves are shifted for convenience of comparison.

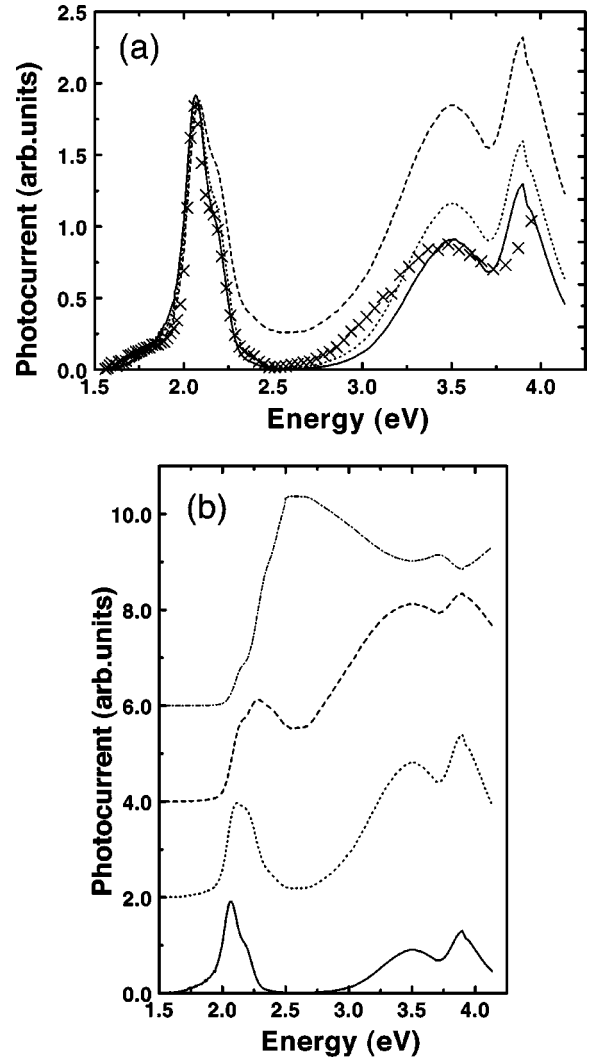


FIG. 7. (a) Comparison of photocurrent action spectrum of Au/P3DDT(2  $\mu$ m)/ITO heterostructure (cross) under illumination through ITO-electrode at  $\pm 10$  V ( $\pm 2.5 \times 10^4$  V/cm) at 130 K with theoretical simulation for different exciton diffusion lengths (5 nm - solid line, 100 nm - dotted line, 200 nm - dashed line); (b) theoretical simulation for exciton diffusion length of 5 nm and different film thicknesses (1.6  $\mu$ m - solid line, 1.0  $\mu$ m - dotted line, 0.5  $\mu$ m - dashed line, and 0.1  $\mu$ m - dash-dotted line). The curves are shifted for convenience of comparison.

0.5  $\mu$ m - dashed line, and 0.1  $\mu$ m - dash-dotted line). This simple model fits experimental data quite satisfactorily using the exciton diffusion length of 5 nm and effective thickness of 1.6  $\mu$ m. The fitting using the expression  $\phi \propto (h\nu - h\nu_0)^2$  for quantum yield<sup>5</sup> produces too high photocurrent at high-photon energy. We must notice here that the fitting is not quantitative because of uncertainties in knowledge of exact function for quantum efficiency on absorption coefficient or energy and some experimental conditions as reflectivity of polymer film and electrodes. But the spectral shape of the photocurrent signal was produced very satisfactorily.

## V. CONCLUSIONS AND SPECULATIONS

We have measured the photocurrent action spectra of the device of Al(Au)/P3DDT/ITO sandwich structure. The pho-

toinjection from ITO and Au electrodes was observed at room temperature. The temperature dependence of J-V characteristics of ITO/P3DDT/Au device have been measured. No polarity effect was found in the ITO/P3DDT/Au device at low temperature. The photoinjection from ITO electrode is not effective at low temperatures. Photoconductivity in ITO/P3DDT/Au sandwich cell at low-electric field and low temperature is an extrinsic process. It is determined by photoinjection of holes from backside Au electrode at positive bias and photoinjection of electrons from the same Au electrode at negative bias. The simple phenomenological model of photoconductivity in poly(3-dodecylthiophene) at low-electric field and low temperatures was proposed.

It is evident that the exciton dissociation at the polymer/ITO and polymer/Au interface is the dominant mechanism of photocurrent generation in poly(3-alkylthiophene) sandwich cell at low electric field. For example, the excellent visible-ultraviolet sensitivity of a Au/poly(3-octyl thiophene)/ITO photodiode<sup>18</sup> at reverse bias voltage could be explained by very effective photoinjection from Au electrode. The quantum yield sufficiently increases at high electric field. But this approach is not appropriate for solar cells. The solar cells based on an interpenetrating polymer network are very promising approach for the improvement of efficiency of polymer solar cells. However, the collection efficiency remains a serious problem in a such approach since the mobilities of charge carriers in disordered polymer systems are low. Recently, it has been shown that the chemical doping of conjugated polymer can be useful in polymer photovoltaic devices.<sup>46</sup> We propose an approach for photoconductivity enhancement in conjugated polymers. This approach is based on our previous results of the study on conjugated polymer - carbon nanotube composites.<sup>47,48</sup> With increase of a volume fraction of a multiwall nanotube (MWNT) in poly(3-hexyl thiophene) the dark conductivity increases drastically at a relatively low concentration of

MWNT (the percolation threshold is only 5.9 vol.% due to high aspect ratio of MWNT). Near the percolation threshold (at about 3 vol.%) we have found the enhancement of photoconductivity of about 25 times in poly(3-hexyl thiophene) - MWNT composites. However, the interaction between MWNT and conjugated polymer is weak.<sup>49</sup> Hence, the enhancement of photoconductivity in this composite was caused only by the improved collection efficiency of charge carriers by highly conducting MWNT.

On the other hand, a conjugated polymer - metal nanoparticles composites could be a promising material for solar cells because of efficient dissociation of excitons at polymer - metal interface. The needlelike conducting particles would be especially interesting because the percolation threshold could be achieved at low concentration. Indeed, we have observed the correlation between the enhanced photoconductivity and the aspect ratio of dopant.<sup>48</sup> It is also known that noble metal nanoparticles absorb light in visible range due to surface plasmons.<sup>50</sup> The increased interaction distance due to light scattering by nanoparticles should also play very important role and make possible the fabrication of thinner solar cells.

#### ACKNOWLEDGMENTS

This work was financially supported by the Research for the Future Program of the Japan Society for the Promotion of Science (Project No. JSPS-RFTF96P00206) and by the Korea Science and Engineering Foundation (KOSEF). The partial support of S. Lee was done by the Ministry of Education (MOE), Korea through the Basic Science Research Institute of Seoul National University. We acknowledge to the Inter-University Center for Natural Science Research of Seoul National University for using the Beckman DU-70 spectrophotometer. We would like also to thank Professor E. Frankevich for helpful discussions.

\*On leave from Heat Physics Department of Uzbek Academy of Science, Tashkent, Uzbekistan. Electronic address: sergey@ele.eng.osaka-u.ac.jp

<sup>1</sup>G. Harrison, J. Grüner, and G.C.W. Spencer, *Phys. Rev. B* **55**, 7831 (1997).

<sup>2</sup>D. Moses *et al.*, *Phys. Rev. B* **54**, 4748 (1996); D. Moses, J. Wang, G. Yu, and A.J. Heeger, *Phys. Rev. Lett.* **80**, 2685 (1998).

<sup>3</sup>M. Yan *et al.*, *Phys. Rev. Lett.* **72**, 1104 (1994); M. Yan, L.J. Rothberg, E.W. Kwock, and T.M. Miller, *ibid.* **75**, 1992 (1994); M. Yan, L.J. Rothberg, E.W. Kwock, and T.M. Miller, *ibid.* **75**, 1992 (1995); J.W.P. Hsu *et al.*, *Phys. Rev. B* **49**, 712 (1994).

<sup>4</sup>H. Antoniadis *et al.*, *Phys. Rev. B* **50**, 14 911 (1994).

<sup>5</sup>S. Barth, H. Bässler, H. Rost, and H.H. Hörhold, *Phys. Rev. B* **56**, 3844 (1997); S. Barth and H. Bässler, *Phys. Rev. Lett.* **79**, 4445 (1997).

<sup>6</sup>E.L. Frankevich *et al.*, *Phys. Rev. B* **53**, 4498 (1996).

<sup>7</sup>A. Köhler *et al.*, *Nature (London)* **392**, 903 (1998).

<sup>8</sup>T.K. Däubler, D. Neher, H. Rost, and H.H. Hörhold, *Phys. Rev. B* **59**, 1964 (1999).

<sup>9</sup>Th. Kugler, M. Lögdlund, and W.R. Salaneck, *IEEE J. Sel. Top. Quantum Electron.* **4**, 14 (1998), and references therein.

<sup>10</sup>M. Yan *et al.*, *Phys. Rev. Lett.* **73**, 744 (1994).

<sup>11</sup>S. Morita, A.A. Zakhidov, and K. Yoshino, *Solid State Commun.* **82**, 249 (1992).

<sup>12</sup>E.L. Frankevich *et al.*, *Phys. Rev. B* **46**, 9320 (1992).

<sup>13</sup>N. Kirova and S. Brazovskii, *Synth. Met.* **85**, 1413 (1997).

<sup>14</sup>J. Cornil, A.J. Heeger, and J.L. Bredas, *Chem. Phys. Lett.* **272**, 463 (1997); J. Cornil *et al.*, *J. Am. Chem. Soc.* **120**, 1289 (1998).

<sup>15</sup>S. Abe, *Synth. Met.* **85**, 1015 (1997).

<sup>16</sup>J. Fagerström and S. Stafström, *Synth. Met.* **85**, 1065 (1997).

<sup>17</sup>K. Yoshino *et al.*, *Solid State Commun.* **69**, 143 (1989); Y. Ohmori, M. Uchida, K. Muro, and K. Yoshino, *ibid.* **80**, 605 (1991); K. Kaneto and K. Yoshino, *Synth. Met.* **28**, 287 (1989).

<sup>18</sup>G. Yu, K. Pakbaz, and A.J. Heeger, *Appl. Phys. Lett.* **64**, 3422 (1994).

<sup>19</sup>M. Berggren *et al.*, *Nature (London)* **372**, 444 (1994).

<sup>20</sup>R. Sugimoto, S. Takeda, H.B. Gu, and K. Yoshino, *Chem. Express* **1**, 635 (1986).

<sup>21</sup>J. Kanicki, in *Handbook of Conducting Polymers*, edited by T. A. Skotheim (Dekker, New York, 1986), Vol. 1, p. 543.

<sup>22</sup>H. Antoniadis *et al.*, *Synth. Met.* **62**, 265 (1994).

<sup>23</sup>R.N. Marks *et al.*, *J. Phys.: Condens. Matter* **6**, 1379 (1994).

<sup>24</sup>X. Wei *et al.*, *Phys. Rev. B* **49**, 17 480 (1994).

<sup>25</sup>K. Yoshino *et al.*, *IEEE Trans. Electron Devices* **44**, 1315 (1997).

- <sup>26</sup>M. Hamaguchi and K. Yoshino, *Jpn. J. Appl. Phys., Part 1* **35**, 4813 (1996).
- <sup>27</sup>*Handbook of Chemistry and Physics* (CRC, Boca Raton, FL, 1988).
- <sup>28</sup>V. Parente *et al.*, *Adv. Mater.* **3**, 319 (1998).
- <sup>29</sup>M. A. Lampert and P. Mark, *Current Injection in Solids* (Academic, New York, 1970).
- <sup>30</sup>M. Liess *et al.*, *Phys. Rev. B* **56**, 15 712 (1997).
- <sup>31</sup>R. Kersting *et al.*, *Phys. Rev. Lett.* **73**, 1440 (1994); W. Graupner *et al.*, *ibid.* **81**, 3259 (1998).
- <sup>32</sup>S. Tasch, G. Kranzelbinder, G. Leising, and U. Scherf, *Phys. Rev. B* **55**, 5079 (1996).
- <sup>33</sup>P.W.M. Blom, M.J.M. de Jong, and M.G. van Munster, *Phys. Rev. B* **55**, R656 (1997).
- <sup>34</sup>D.D.C. Bradley, and R.H. Friend, *J. Phys.: Condens. Matter* **1**, 3671 (1989).
- <sup>35</sup>C.H. Lee, G. Yu, and A.J. Heeger, *Phys. Rev. B* **47**, 15 543 (1993).
- <sup>36</sup>V.I. Arkhipov, E.V. Emelianova, and H. Bässler, *Phys. Rev. Lett.* **82**, 1321 (1999).
- <sup>37</sup>H. Killesreiter and H. Bässler, *Phys. Status Solidi B* **51**, 657 (1972).
- <sup>38</sup>K. Yoshino *et al.*, *Jpn. J. Appl. Phys., Part 2* **32**, L357 (1993).
- <sup>39</sup>V. Choong *et al.*, *Appl. Phys. Lett.* **69**, 1492 (1996).
- <sup>40</sup>H. Becker, S.E. Burnes, and R.H. Friend, *Phys. Rev. B* **56**, 1893 (1997).
- <sup>41</sup>J.C. Scott *et al.*, *J. Appl. Phys.* **79**, 2745 (1996).
- <sup>42</sup>A.R. Schlattmann *et al.*, *Appl. Phys. Lett.* **69**, 1764 (1996).
- <sup>43</sup>A.K. Ghosh and T. Feng, *J. Appl. Phys.* **49**, 5982 (1978).
- <sup>44</sup>N.T. Binh, M. Gailberger, and H. Bässler, *Synth. Met.* **47**, 77 (1992).
- <sup>45</sup>R. Kersting *et al.*, *Phys. Rev. Lett.* **70**, 3820 (1993).
- <sup>46</sup>A.C. Arias *et al.*, *Phys. Rev. B* **60**, 1854 (1999).
- <sup>47</sup>K. Yoshino, H. Kajii, H. Araki, T. Sonoda, H. Take, and S.B. Lee, *Fullerene Sci. Technol.* **7**, 695 (1999).
- <sup>48</sup>S. B. Lee, H. Araki, H. Kajii, T. Sonoda, A. Fujii, and K. Yoshino, in *Proceedings of the Third Symposium on Atomic-Scale Surface and Interface Dynamics, Fukuoka, Japan, 1999*, edited by T. Nishinaga (University of Tokyo, Tokyo, 1999), p. 97.
- <sup>49</sup>S. Curran *et al.*, *Adv. Mater.* **10**, 1091 (1998).
- <sup>50</sup>See, for example, H. Inouye *et al.*, *Phys. Rev. B* **57**, 11 334 (1998).